

## Anisotropic Cardiac Conduction

Irum Kotadia,<sup>1,2</sup> John Whitaker,<sup>1,2</sup> Caroline Roney,<sup>1</sup> Steven Niederer,<sup>1</sup> Mark O'Neill,<sup>1,2</sup> Martin Bishop<sup>1</sup> and Matthew Wright<sup>1,2</sup>

1. School of Biomedical Engineering and Imaging Sciences, King's College, London, UK; 2. Guy's and St Thomas' NHS Foundation Trust, London, UK

### Abstract

Anisotropy is the property of directional dependence. In cardiac tissue, conduction velocity is anisotropic and its orientation is determined by myocyte direction. Cell shape and size, excitability, myocardial fibrosis, gap junction distribution and function are all considered to contribute to anisotropic conduction. In disease states, anisotropic conduction may be enhanced, and is implicated, in the genesis of pathological arrhythmias. The principal mechanism responsible for enhanced anisotropy in disease remains uncertain. Possible contributors include changes in cellular excitability, changes in gap junction distribution or function and cellular uncoupling through interstitial fibrosis. It has recently been demonstrated that myocyte orientation may be identified using diffusion tensor magnetic resonance imaging in explanted hearts, and multisite pacing protocols have been proposed to estimate myocyte orientation and anisotropic conduction *in vivo*. These tools have the potential to contribute to the understanding of the role of myocyte disarray and anisotropic conduction in arrhythmic states.

### Keywords

Anisotropy, anisotropic conduction, arrhythmias, pacing, conduction velocity

**Disclosure:** The research was supported by the National Institute for Health Research (NIHR) Clinical Research Facility at Guy's and St Thomas' NHS Foundation Trust and NIHR Biomedical Research Centre based at Guy's and St Thomas' NHS Foundation Trust and King's College London. The views expressed are those of the authors, and not necessarily those of the NHS, the NIHR or the Department of Health. JW is supported by a Medical Research Council UK Clinical Research Training Fellowship (grant code: MR/N001877/1). The authors have no other conflicts of interest to disclose.

**Received:** 15 February 2020 **Accepted:** 9 October 2020 **Citation:** *Arrhythmia & Electrophysiology Review* 2020;9(4):202–10.

**DOI:** <https://doi.org/10.15420/aer.2020.04>

**Correspondence:** John Whitaker, School of Biomedical Engineering and Imaging Sciences, King's College London, Strand, London WC2R 2LS, UK. E: [john.whitaker@kcl.ac.uk](mailto:john.whitaker@kcl.ac.uk)

**Open Access:** This work is open access under the CC-BY-NC 4.0 License which allows users to copy, redistribute and make derivative works for non-commercial purposes, provided the original work is cited correctly.

Anisotropy is the property of directional dependence. In cardiac tissue, conduction velocity (CV) is anisotropic, that is, the magnitude of CV depends on the direction of a wave of activation. Anisotropic conduction facilitates prompt and synchronised cardiac chamber activation. In disease states, anisotropic conduction is implicated in the genesis of pathological arrhythmias. It can determine unidirectional conduction block (UCB), which is a prerequisite for re-entry, the likelihood of propagation of ectopic foci of activation and the motion and stability of re-entrant activation patterns. The response of cardiac tissue to treatment, such as pacing, and the ability of a high-voltage stimuli to terminate fibrillation through the generation of virtual electrodes are dependent on the anisotropic properties of the myocardium.<sup>1,2</sup> Therefore, anisotropic conduction is an important property of cardiac tissue, disease and response to treatment of arrhythmias. In the present study, we discuss the mechanisms determining anisotropic conduction within cardiac tissue, the contribution of anisotropic conduction to the mechanisms underlying pathological re-entrant arrhythmias and the reported options for assessing anisotropy.

### Factors Responsible for Anisotropic Conduction

CV varies in different locations within the heart. The magnitude of CV within cardiac tissue demonstrates directional dependence, that is, anisotropy, with the maximum speed of conduction being observed parallel to the direction of myocytes (longitudinal CV) and the slowest

speed of conduction perpendicular to the myocytes (transverse CV).<sup>3,4</sup> A further layer of complexity arises when conductivity is considered in three dimensions. At a cellular level, myocytes are transversally isotropic, that is, CV is equal in any direction in the plane perpendicular to the principal axis of the myocyte; however, this does not hold true when conduction is considered at the tissue scale, where the laminar structure of the tissue results in orthotropic conduction, that is, variation in conductivity in each of the three dimensions.<sup>5,6</sup> Much of the literature pertaining to anisotropic conduction makes the assumption, often implicitly, of transverse isotropy of conduction, which must be considered a limitation in light of these data regarding orthotropy. However, having acknowledged this limitation, the consideration of anisotropy in two dimensions yields important data. The ratio between the maximum and minimum CV observed is known as the 'anisotropy ratio' ( $AR_{CV}$ ) and indicates the magnitude of CV anisotropy within that tissue. Other characteristics of cardiac tissue also demonstrate anisotropy, including the conductivity of tissue (a parameter that is frequently considered in cardiac modelling studies) and the physical structure of the tissue.<sup>7,8</sup>

Several factors have been identified that contribute to CV anisotropy. These include cell size, cell shape and gap junction distribution. Various experimental setups have been established to attempt to separately measure longitudinal and transverse CV.<sup>9</sup> One of the challenges in

doing so has been to separate the impact of intrinsic tissue anisotropy from the impact of wavefront curvature, which has a profound effect on CV and is influenced by anisotropy.<sup>10</sup> The impact of wavefront curvature presents significant challenges for the assessment of  $AR_{CV}$  *in vivo*.<sup>9</sup> Along with the complex 3D alignment of myocytes within the human heart, these challenges have prevented routine assessment of  $AR_{CV}$  within intact cardiac chambers.<sup>11</sup>

### Cell Shape and Size

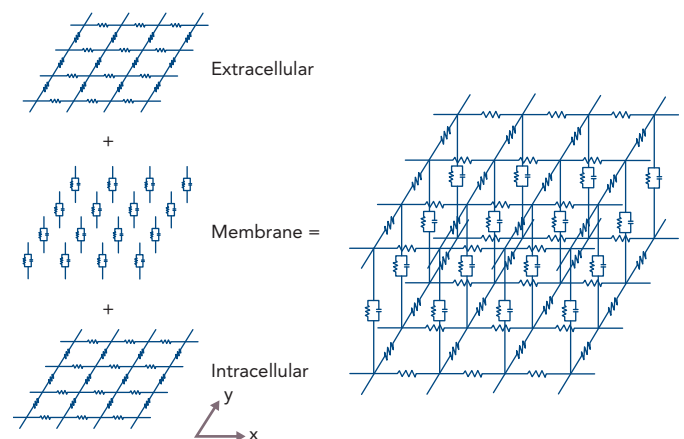
Cardiac myocytes are elongated cells with a cylindrical shape. They are oriented in bundles of parallel cells that then form into laminar sheets, rendering the microstructural architecture of human cardiac tissue anisotropic.<sup>12</sup> Early experimental observations on the anisotropic nature of cardiac conduction noted myocyte orientation as the principal determinant of the direction of the maximal CV observed.<sup>13</sup> In addition to experimentally demonstrating anisotropic conduction of the myocardium, Clerc also highlighted the presence of unequal resistivity anisotropy ratios in the intra- and extra-cellular domains, which was confirmed in subsequent studies.<sup>13,14</sup> This key observation prompted further experimental and theoretical work in the coming years with significant implications for understanding complex propagation and polarisation patterns in 2D and 3D cardiac tissue, and was instrumental in the development of the bidomain model of cardiac electrophysiology (Figure 1).<sup>15–19</sup>

As demonstrated in Figure 2, a wave of conduction travelling perpendicular to the principal axis of a myocyte (transverse direction) will meet a greater number of cellular interfaces per unit length than will be encountered in the direction parallel to myocyte direction (longitudinal direction). Cytoplasmic conduction along the length of the myocyte is rapid with low resistance, whereas low-velocity, high-resistance conduction occurs across the gap junctions that electrically couple adjacent cells. This distinction is an important determinant of CV anisotropy. When isolated single chains of myocytes are considered, conduction slowing at cellular junctions results in discontinuous or saltatory conduction, and >50% of conduction time may occur at the small distance across gap junctions, with the remainder of conduction time being due to cytoplasmic conduction.<sup>20,21</sup> However, Figure 2 further demonstrates the reduction of this effect in 2D laminar tissue due to lateral cell connections that permit divergence of the local excitatory current around the junction, effectively speeding up conduction across the cellular interface.<sup>21</sup> Considering propagation in the longitudinal direction, it is also evident that a depolarising wave travelling in a longer cell will encounter a lower frequency of cellular interfaces than a wave travelling in a shorter cell, with a consequent increase in longitudinal CV in longer cells, and therefore, anisotropy. Experimental and modelling studies indicate that pathological changes in cell shape and size affecting the length–width ratio will have a consequent impact on anisotropy of conduction.<sup>22</sup> Computational simulation of the activation of representative blocks of tissue confirms maximum propagation speed along the axis of myocytes, but also reveals additional levels of complexity to propagation patterns in 3D.<sup>5,6</sup>

### Myocardial Fibrosis

Myocardial fibrosis is a common consequence of many human cardiac pathologies, and may be classified as reactive fibrosis, which is the result of increased collagen deposition, or replacement fibrosis ('scar'), in which collagen replaces injured myocytes.<sup>23,24</sup> Collagen deposition may be in the form of discrete regions of dense collagen without any viable myocytes ('compact' fibrosis), an increase in the

**Figure 1: Resistor Network Demonstrating a 2D Bidomain Model**



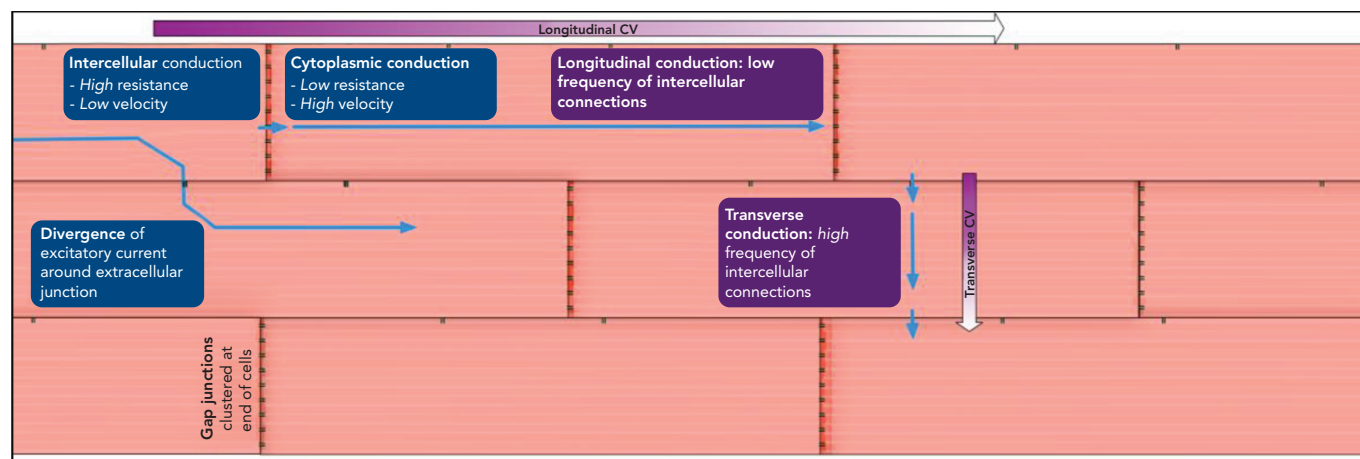
The x and y planes are represented by the intracellular and extracellular spaces (bi-domains) in the form of a 2D resistor network. These planes are coupled vertically by resistors and capacitors that represent the membrane and together form a model for a single layer of cells. However, resistors in the x and y directions may be unequal. Anisotropic ratio in the extracellular domain is estimated at 2, compared with the intracellular domain that is estimated at 10. Source: Roth et al. 1992.<sup>19</sup> Reproduced with permission from Springer Nature.

extracellular matrix ('interstitial' fibrosis) or due to an intermingling of myocytes and stretches of collagen fibres.<sup>24</sup> Different patterns of fibrosis appear to affect conduction and conduction anisotropy differently. Interstitial fibrosis, predominantly separating the longitudinal cellular bundles, results in the most pronounced decrease in transverse CV in the human heart, and an increase in  $AR_{CV}$ .<sup>25</sup> In this situation, enhanced microstructural discontinuities (observed in an animal model under experimental conditions) result in dissociated conduction with longer conduction times and a zigzag pattern, as well as promoting non-uniform action potential properties.<sup>26–28</sup> These characteristics of transverse conduction are due to the tortuous route that a propagating wave must traverse, in addition to electrical uncoupling in the transverse direction, due to increased interstitial resistance to current flow.<sup>29</sup> These changes amplify the  $AR_{CV}$  of tissue, which favours the initiation of re-entry and will be discussed later.<sup>4</sup>

### Gap Junctions

Gap junctions electrically couple adjacent cells by behaving as selectively permeable ion channels. The conductivity of gap junctions (a factor of the density of gap junctions and their individual behaviour) is a major determinant of intercellular resistivity. This in part determines CV, affecting the extent of delay encountered at the intercellular junction. Gap junctions cluster at the longitudinal end of myocytes, but are also found along the length of cells, electrically coupling cells in the transverse direction.<sup>30</sup> Pathologically, the redistribution of gap junctions can result in a decrease in density of gap junctions at the longitudinal cell ends, and an increase along the shaft of the cells, known as 'lateralisation'.<sup>30</sup> Furthermore, an overall reduction in the expression of gap junctions can be seen in ventricular tissue. These findings have been observed in a range of pathological processes associated with arrhythmia, including dilated cardiomyopathy and ischaemic cardiomyopathy.<sup>31,32</sup> When the gap junction protein Cx43 was reduced by 95% in a murine experimental model, ventricular tissue demonstrated decreased CV and increased  $AR_{CV}$ , which resulted in greater susceptibility to ventricular arrhythmias.<sup>33</sup> Full-thickness gap junction distribution disturbance was seen in an early post-infarct canine myocardium in which ventricular tachycardia (VT) was inducible and co-localised with the central common isthmus of these VT circuits,

**Figure 2: Cellular Features that Contribute to Conduction Velocity Anisotropy in Myocardial Tissue with Long, Cylindrical Cells**



Fast longitudinal conduction results from rapid, low-resistance cytoplasmic conduction interrupted by infrequent high-resistance, low-velocity intercellular conduction, which is facilitated by clustering of gap junctions at cell ends. Reduced conduction slowing at intercellular junctions results from divergence of local excitatory current around intercellular connections. Slow transverse conduction results from a high frequency of high resistance, low-velocity intercellular junctions with fewer gap junctions. CV = conduction velocity.

while only partial-thickness distribution abnormalities were observed in non-inducible hearts. In atrial tissue, genetically determined reduction in Cx40 and Cx43 function has been identified in patients with AF in the absence of any predisposing conditions. Furthermore, experimentally promoting Cx43 expression in a porcine model of AF restored CV, with a resultant decrease in susceptibility to AF.<sup>34–37</sup> While these observations suggest that pathological changes in gap junction behaviour would be an important determinant of changes in CV and CV anisotropy in disease, other experimental evidence suggests that it has a relatively modest impact on changes in CV anisotropy.<sup>22</sup> This may reflect an excess of gap junctions, providing a buffer that minimises the impact of redistribution and differences in function (conductivity) of the redistributed gap junctions in the pathological state. The surrogates used to identify the distribution of gap junctions (usually done through immunohistochemical analysis of the localisation of Connexin proteins) may also not accurately identify the location of the functional gap junction components.<sup>30,38</sup> Resolving the discrepancy between the observation of remodelled gap junctions in clinical conditions associated with arrhythmia against experimental evidence suggesting a modest impact on CV with the observed changes in gap junction distribution has remained challenging. A further possible explanation may be the potentiation of changes in gap junction effects by increases in interstitial volume. In an experimental model of increased interstitial volume (which is observed in a broad range of cardiovascular pathologies), gap junction blockade resulted in slowed conduction and increased  $AR_{CV}$ , which was associated with an increased susceptibility to arrhythmia that was not seen in controls.<sup>39,40</sup> Outstanding issues remain surrounding the magnitude of the effect in gap junction remodelling and other conditions required to unmask the arrhythmogenic effects. However, current data suggest that the consequence of changes in gap junction function in disease predispose to arrhythmia in a range of conditions.

## Functional Determinants of Anisotropy

In addition to structural determinants of CV and  $AR_{CV}$ , there are important functional contributors to these characteristics. The high density of sodium channels found at the intercalated discs between myocytes represents an important modifier of conduction at the intercalated discs, and thus, conduction along the axis of the myocyte.<sup>41,42</sup> Activation of the

sympathetic nervous system increases longitudinal CV, but not transverse CV, therefore increasing  $AR_{CV}$  in a porcine ventricular myocardium. This effect was shown to be abolished by gap junction blockade, demonstrating the importance of the functional modulation of anisotropic conduction.<sup>43</sup>

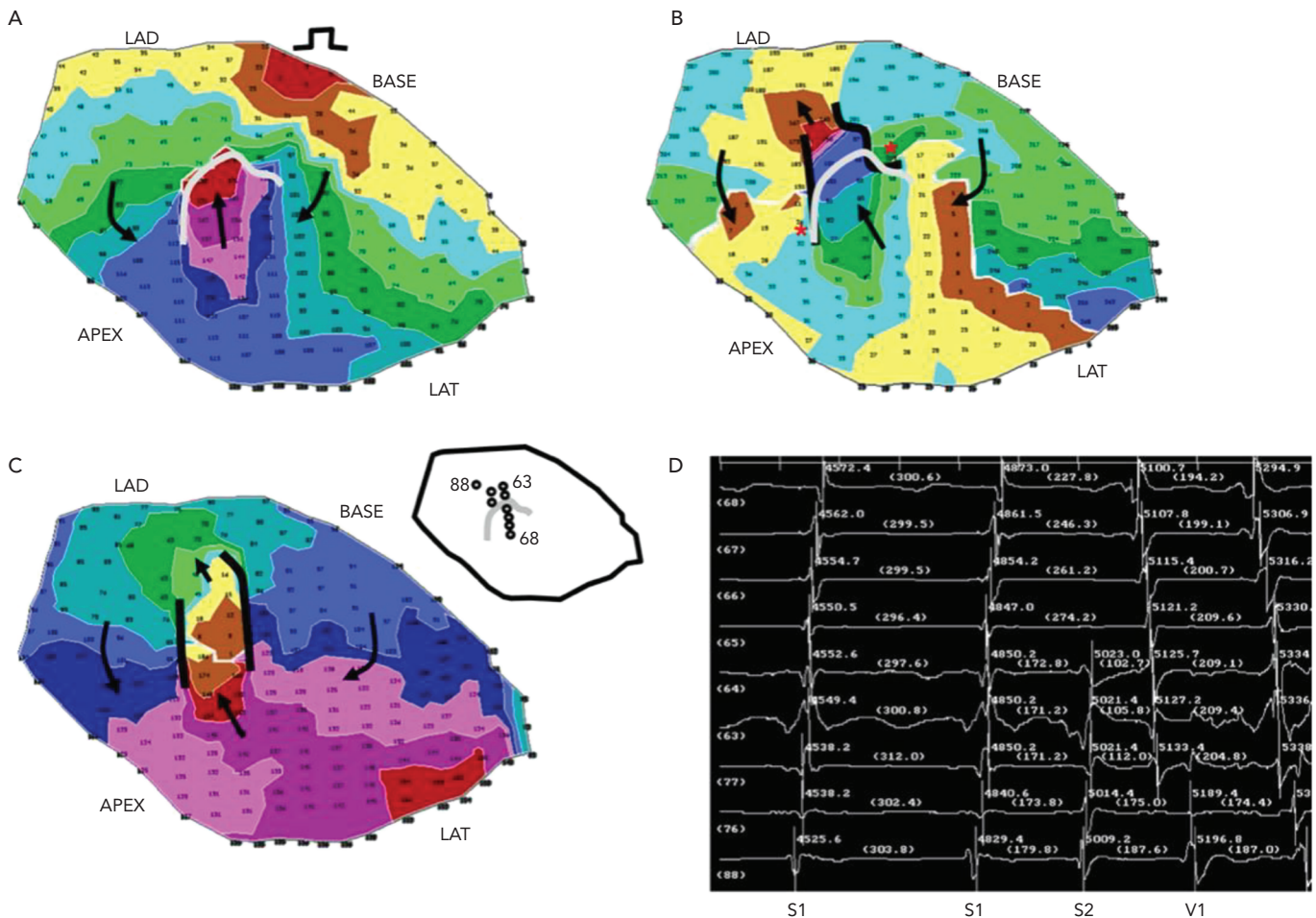
The clinical significance of alterations in sodium channel function is demonstrated through the loss of function mutations of the sodium channel protein type 5 subunit alpha (*SCN5A*) gene, resulting in reduced CV, as is seen in Brugada and Lev-Lenègre syndromes. Prior *in vivo* studies have demonstrated that reduced CV in the context of normal heterogeneities within the right ventricle predisposes to vulnerabilities of re-entrant tachycardias that may precipitate ventricular fibrillation, and consequently, sudden cardiac death.<sup>44</sup>

More recently, a reduction in the number of cardiac sodium channels was shown using immunocytochemistry of cardiac tissue from patients with a diagnosis of arrhythmogenic right ventricular cardiomyopathy (ARVC).<sup>45</sup> The same study also demonstrated reduced signal of the gap junction protein Cx43, previously discussed as an important determinant of changes in CV and CV anisotropy in disease. These observations likely contribute to the increase in arrhythmia vulnerability seen in ARVC.

## Variations in Anisotropic Ratio and Conduction Velocity in the Heart Atrium

Specific regions of preferential conduction within the atria appear to be optimised for conducting a wave of depolarisation to facilitate an orderly sequence of activation in the atria. These regions include the crista terminalis, running from the sinus node to the eustachian valve and giving off trabeculations that facilitate right atrial activation and left atrial activation via Bachmann's bundle.<sup>46</sup> These regions demonstrate both faster CV and increased  $AR_{CV}$  (in some cases transverse conduction is absent) than in surrounding atrial tissue.<sup>47,48</sup>  $AR_{CV}$  of up to 10 has been recorded in these regions.<sup>49</sup> In the crista terminalis, pronounced anisotropy fulfils the functional requirement of permitting appropriate timing of atrial activation.  $AR_{CV}$  in atrial body tissue has been less commonly reported, but in preclinical and clinical experiments where it has been quantified, it is lower than that recorded in either the crista terminalis or Bachmann's bundle.<sup>50,51</sup>

Figure 3: Activation Maps of the Epicardial Surface of The Anterior Left Ventricle Following a Premature Extra-stimulus from the Base of the Left Ventricle



Grey line indicates a line of unidirectional block that has occurred at the infarct border zone. A: Activation map demonstrates bifurcation of the wavefront of depolarisation around the line of unidirectional block, which pivots around the line of unidirectional block to activate it from the opposite direction. B: Depolarisation of the adjacent tissue that has now had time to repolarise, and which completes the first cycle of re-entry. C: Resulting ventricular tachycardia that ensues. Source: Ciaccio et al. 2015.<sup>54</sup> Reproduced from Elsevier under a Creative Commons (CC BY) licence.

Myocytes in the heart demonstrate patterns of organisation that may be seen when tissue is examined macroscopically.

### Ventricular Tissue

The highest speeds of conduction found within the heart are in His-Purkinje tissue.<sup>52</sup> These insulated cells are optimised for rapid longitudinal conduction of a depolarising wave exiting the atrioventricular node to a large mass of ventricular tissue.<sup>53</sup> The rapid dispersion of a wave of activation permits synchronized ventricular contraction, obviating the need for rapid conduction between ventricular myocytes, and therefore, overcoming the relatively slow conduction between adjacent ventricular myocytes. The insulation of these tracts by a fibrous sheath prevents dispersion of current in a transverse direction (beyond the strand enclosed in a fibrous sheath).<sup>54</sup> In contrast, CV in ventricular tissue is among the slowest within the heart and demonstrates a correspondingly low anisotropy ratio ( $AR_{CV}$ ). Under experimental conditions, mammalian ventricular tissue has a maximum longitudinal CV around 0.5–0.6  $ms^{-1}$ , whereas transverse CV is estimated between 0.15 and 0.2  $ms^{-1}$ , and thus the anisotropy ratio is between 2.5 and 4.<sup>13,55</sup> In ventricular tissue, myocyte orientation seems to be optimised for mechanical efficiency, rather than for rapid dispersion of a wave of activation, which is instead facilitated by the cardiac conduction system tissue that rapidly disperses the wave of depolarisation, resulting in synchronised ventricular contraction.<sup>56</sup>

### Anisotropic Conduction as a Substrate for Arrhythmia

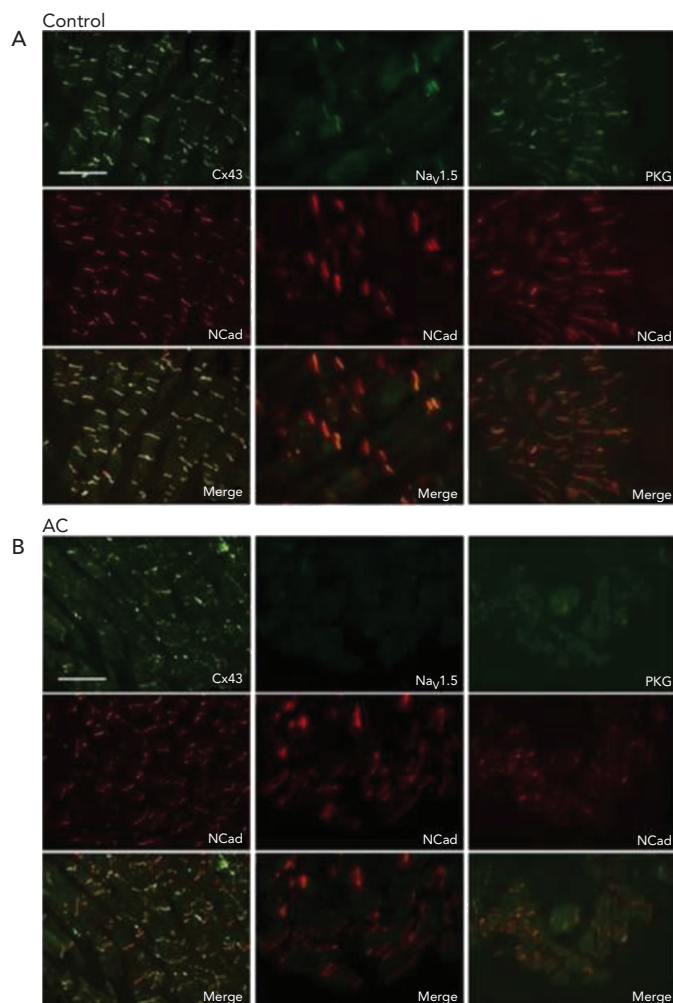
Re-entry is a key mechanism underlying the majority of clinically important arrhythmias responsible for affecting patient prognosis or symptom burden. This may take the form of a stable and mappable re-entrant circuit, such as those seen in post-infarct VT, or may be a complex interaction of one or more unmappable re-entrant circuits, such as those seen in AF, the exact nature of which remains to be definitively established. Despite ongoing uncertainty surrounding the activation patterns in AF, it is acknowledged that re-entrant activation of the atria plays a key role.

### Variations in Anisotropic Ratio and Conduction Velocity in the Pathological Heart

Examples of enhanced  $AR_{CV}$  in pathological conditions have been reported, including during right atrial assessment in patients with chronically stretched atria secondary to mitral stenosis, who demonstrated increased  $AR_{CV}$  at the crista terminalis compared to controls. This represents an example of pathological substrate remodelling in patients with a condition associated with a high incidence of AF.<sup>57</sup> A similar increase in CV anisotropy has been observed in atrial tissue from patients undergoing surgical AF ablation.<sup>58</sup> Optical mapping has demonstrated heterogeneously decreased CV and increased  $AR_{CV}$  within left ventricular tissue from end-stage heart failure patients, as well



**Figure 4: Immunohistochemical Analysis Demonstrating Pathological Remodelling in Arrhythmogenic Right Ventricular Dysplasia**



Immunohistochemical analysis was performed on post-mortem biopsies from five control patients and five patients with a history of arrhythmogenic right ventricular dysplasia (ARVC). Further biopsies were taken from the right ventricular septum in 15 ARVC patients. A: Control patients. (B) Patients with ARVC. Panels show a reduction in immunoreactive signal intensity of Cx43 (left), Na<sub>v</sub>1.5 (middle), and PKG (right) at the intercalated discs in ARVC patients compared with control patients. N-cadherin (NCad) is a cell-adhesion molecule that has no known human mutations and resides at the intercalated discs. Samples were double stained. Double-labelling was performed with NCad to validate the results. Source: Noorman et al. 2013.<sup>45</sup> Reproduced with permission from Elsevier.

as the increased incidence of transverse conduction block, reflecting substrate changes that may contribute to the increased incidence of re-entrant arrhythmia in this group.<sup>59</sup> High-resolution activation mapping of post-infarct VT circuits in a porcine model suggest that extreme slowing of conduction perpendicular to the isthmus is present, with relatively normal CV within the isthmus, in a pronounced example of anisotropic conduction during a sustained arrhythmia.<sup>60</sup>

## Unidirectional Conduction Block

UCB is a prerequisite for the development of re-entry.<sup>61</sup> A variety of mechanisms may give rise to UCB, including functional asymmetry of the cardiac action potential, local heterogeneity of tissue excitability and discontinuities in tissue structure. Simulation studies demonstrate that local excitation within a homogeneous excitable media may interact with the tail of a preceding wave of depolarisation and result in UCB. In order to do so, the local excitation must be critically timed to fall within a vulnerable window, which may be defined in terms of membrane voltage,

time or space.<sup>62</sup> While UCB may occur in homogeneous media due to the intrinsic asymmetry of the action potential (termed 'functional heterogeneity'), the width of the vulnerable window may be significantly expanded by heterogeneity of the electrical properties of tissue, including the availability of Na<sup>+</sup> channels (excitability), cell-to-cell coupling (connectivity) and the behaviour of K<sup>+</sup> channels (repolarisation).<sup>63</sup> Furthermore, structurally determined source-sink mismatch at the transition from a small to a large mass of excitable tissue may also give rise to UCB, as propagation fails in the direction of a rapidly expanding volume of excitable tissue.<sup>64</sup> The anisotropic behaviour of tissue has been demonstrated to promote UCB. In post-infarct VT, re-entrant circuits may be established by the appearance of an arc of conduction block, with subsequent activation of tissue distal to the initial arc sufficiently late that it has recovered excitability and depolarisation can occur (Figure 3).<sup>65,66</sup> If an arc of conduction block occurs in the longitudinal direction relative to myocyte orientation, that is, in the direction of maximal CV, slower conduction occurs in the transverse direction (a function of the intrinsic difference between transverse CV and longitudinal CV due to tissue anisotropy, as well as wavefront curvature introduced by the arc of block). This allows additional time for recovery of excitability of tissue distal to the arc, such that re-entry is more likely to be established than if the initial arc of conduction block was in the transverse direction.<sup>55</sup> Similar re-entrant patterns have been demonstrated in atrial tissue, identifying anisotropy of conduction as a key mechanism promoting re-entry.<sup>67</sup> Recently, Anter et al. used high-resolution mapping of re-entrant VT circuits to show that a key substrate in the sustenance of the arrhythmia was conduction slowing at the entrance/exit of the VT isthmus.<sup>60</sup> An important component of this was the highly curved nature of the wavefront propagation in these regions, transitioning from parallel to the faster fibre orientation (along the isthmus direction) to propagate transverse to it in order to loop back around and re-enter.<sup>60</sup>

## Robustness of Conduction

The effect of pathological remodelling on the robustness of conduction, quantified as 'safety factor', and indicating under what circumstances conduction will fail, remains uncertain, although alterations in mechanical and electrical coupling of cells at the intercalated discs have been postulated as potential mechanisms. Figure 4 demonstrates disturbance in the immunoreactive signals of connexin 43 and sodium channels following pathological remodelling of the right ventricle in patients ARVC. These changes have previously been found to be associated with reduced CV, and have an increased susceptibility to the initiation and perpetuation of arrhythmias.<sup>45</sup> Theoretical studies and experimental data suggest that uncoupling cells in the transverse direction may result in extremely slow yet robust conduction, an effect which would promote the development of re-entry.<sup>49,68</sup> Other investigators have demonstrated more robust conduction in the longitudinal direction under experimental conditions as a result of cellular uncoupling.<sup>69</sup> In fibrotic human left ventricular tissue, transverse conduction block was seen more frequently than longitudinal block.<sup>59</sup> Differences in methodology may explain some of the discrepancies in the results, and it is possible that different mechanisms of remodelling have different effects on transverse conduction safety. At present, the existence of a consistent effect of pathological remodelling on the differences in robustness of conduction in the longitudinal versus the transverse direction remains uncertain.

## Anisotropic Re-entry

In addition to UCB, re-entrant circuits characteristically require a region of inexcitability for the re-entrant wave to circumnavigate. This may take the form of a fixed anatomic obstacle to conduction, such as a valve or blood

vessel, or if occurring in the absence of such an obstacle, can be termed 'functional re-entry'. Functional re-entrant circuits have been observed experimentally.<sup>70</sup> Originally, this was explained by the 'leading circle' concept, whereby the central region of the re-entry circuit is activated by multiple wavelets branching from the main re-entry circuit (*Figure 5*). Experimental data indicate that this functional re-entry may arise due to heterogeneity in the refractory properties of the tissue, but may also arise in the absence of marked differences in refractoriness, exclusively due to anisotropic tissue properties of conduction.<sup>28,71</sup> Modelling studies have suggested that functional re-entry within the pulmonary veins may underlie rapid activation that results in paroxysms of AF, which in the present study was dependent on heterogeneous and anisotropic conduction within the pulmonary veins.<sup>72,73</sup> CV anisotropy therefore represents a distinct mechanism underlying sustained functional re-entry. In an experimental setting, the re-entrant path of these anisotropic re-entrant circuits is closely related to myocyte orientation.<sup>74</sup>

### Spiral Wavebreak

Junctions in myocyte orientation are observed at typical places in the atria (an example of myocardial arrangement is shown in *Figure 6*), and represent locations where the propagation of a spreading wavefront is subject to changes in CV and anisotropy.<sup>75</sup>

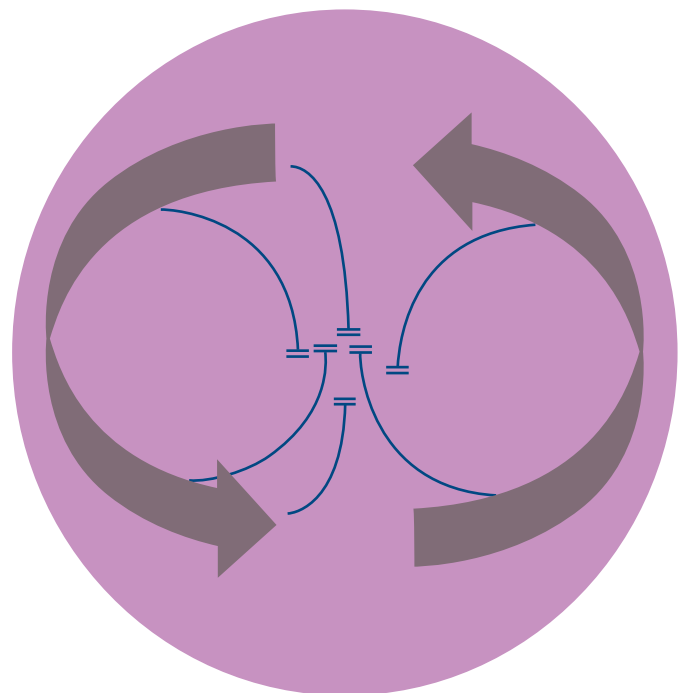
In 3D tissue, spiral waves manifest as a scroll wave or vortex. The break-up of a scroll wave is a potential mechanism underpinning a transition from a tachycardia to fibrillation. The centre of the scroll or filament forms a line through the centre of the scroll analogous to the phase singularity in 2D spiral waves. The relationship between CV anisotropy and filaments has predominantly been investigated using mathematical models. Mathematical formulations and simulation studies have shown that the motion of scroll wave filaments is determined by local anisotropy.<sup>76</sup> Simulations have predicted that tissue anisotropy promotes filament motion towards the apex in the ventricles.<sup>77</sup> In addition, simulations have shown that spatially varying anisotropy promotes both bending of the filament and slow wave speed due to curvature, which can contribute to wavebreak.<sup>78</sup> The stability and location of scroll waves in cardiac tissue are highly dependent on tissue CV anisotropy.

Spiral waves (in 2D) or scroll waves (in 3D) are examples of functional re-entrant circuits that are thought to be involved in the mechanisms underlying AF and VF, and have been observed more frequently in ventricular locations at abrupt junctions of myocyte orientations.<sup>79–82</sup> Furthermore, junctions where myocytes meet in different directions are regions that favour the development of UCB, as well as promoting wavebreak, which is observed in fibrillation and may be a mechanism by which fibrillation is sustained.<sup>83,84</sup> These considerations illustrate the importance of myocyte orientation and anisotropic conduction properties in the development and maintenance of functional myocardial re-entrant circuits, and suggest mechanisms that may promote fibrillation.

### Ectopic Foci

In addition to promoting re-entry, anisotropy of conduction has been implicated in arrhythmia initiation through the propagation of wavefronts from ectopic foci of depolarisation. In simulation studies, a critical degree of cellular uncoupling related anisotropy, for example, that which may be seen with myocardial fibrosis, will permit propagation of an ectopic wavefront, which would otherwise extinguish.<sup>85</sup> Ectopic foci are well known to play a crucial role in the initiation of clinical arrhythmias, including AF.<sup>73</sup>

**Figure 5: Functional Re-entry Circuit Demonstrating the Leading Circle Concept**

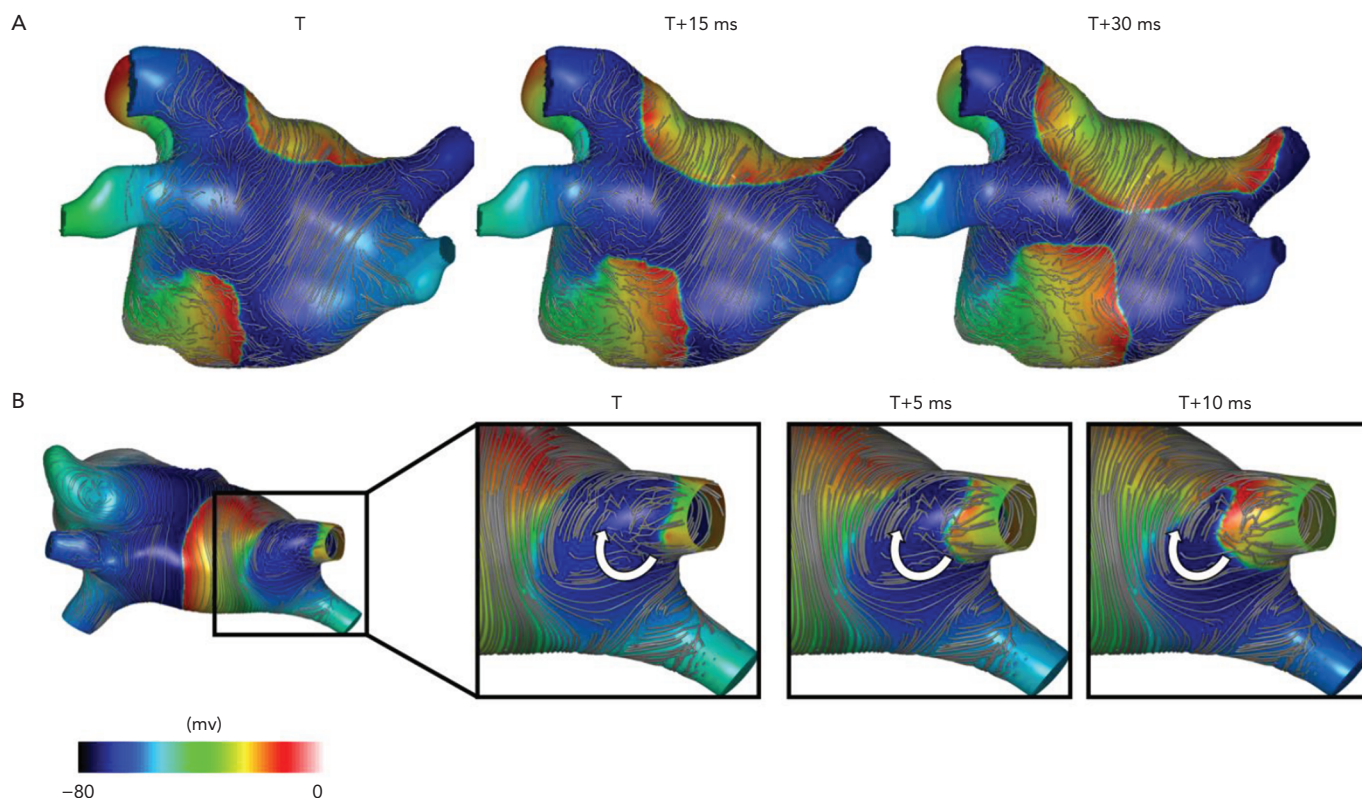


Black arrows represent the re-entry circuit, and blue lines represent centripetal wavelets activating the central region of the circuit. Wavelets are extinguished prior to passing the centre point, and are therefore, unable to shortcut the circuit.

### Outstanding Questions

CV anisotropy is a characteristic of myocardial tissue. The speed of conduction is reliably greatest in the direction parallel to the longitudinal orientation of myocytes. As such, there is an intimate duality between conduction anisotropy and myocyte orientation. Both CV and  $AR_{CV}$  change following pathological tissue remodelling and are associated with pro-arrhythmic states. Uncertainty remains regarding the magnitude of the change, which is likely to depend on the location and pathological process considered. There are compelling explanations and experimental evidence demonstrating mechanisms by which changes in anisotropy may promote re-entry. Some of the discrepancies in the available evidence relate to the experimental models used. Most data have been collected in experimental models due to the difficulty of assessing both myocyte orientation and anisotropy *in vivo*, and as such, there is residual uncertainty as to the translatability of specific experimental results to human physiology. Recently, an estimation of human atrial myocyte orientation in *ex vivo* hearts has been made, establishing that through the use of diffusion-tensor MRI (DT-MRI), myocyte orientation of both epicardial and endocardial atrial tissue layers may be estimated, which was previously only possible through direct tissue examination.<sup>86</sup> Furthermore, recent reports have successfully demonstrated that DT-MRI may be reproducibly applied *in vivo*. It has been used to demonstrate myocyte disarray in hypertrophic cardiomyopathy patients and has been correlated with the incidence of ventricular arrhythmias.<sup>87,88</sup> In this case, decreased structural anisotropy (when averaged over the imaged voxel volume), representing myocyte disarray, was associated with an increased incidence of ventricular arrhythmias. Importantly, the identification of decreased averaged structural anisotropy must be distinguished from the conduction characteristics of myocardium in hypertrophic cardiomyopathy, which remains highly anisotropic in fibrotic areas.<sup>25</sup> It is hoped that DT-MRI application to other pathologies associated with myocyte disarray and arrhythmias will follow and further define the

Figure 6: Atrial Fibre Atlas and Activation Pattern



A: Atrial fibre atlas constructed from a high-resolution diffusion tensor MRI dataset from which myocyte orientation (grey lines) was derived. In an electrophysiological simulation, wavefronts are seen propagating up and down the posterior wall. Roof of the atrium, which contains myocytes oriented in parallel, demonstrates rapid wavefront progression. Lower posterior wall, in which there is myocyte disarray, demonstrates slower and less uniform progression of the wavefront. B: Same model as A is shown. In this simulation, the model was paced at a cycle length of 155 ms for five beats from the right superior pulmonary vein rim during sinus rhythm to represent a train of ectopics. The figure shows the activation map of the fifth ectopic beat, which leads to spiral wave re-entry. Planar wavebreak leading to re-entry at the junction of the left atrium and right superior pulmonary vein is seen.

structural characteristics of the myocardium in pathological conditions. An alternative approach to *in vivo* imaging has been proposed to establish both myocyte orientation and  $AR_{CV}$  in the human atrium using activation patterns during pacing from multiple sites in a process designed to overcome the challenges of wavefront curvature and propagation of wavefronts non-parallel or perpendicular to myocyte orientation (Figure 6).<sup>89</sup> If validated, such a tool may facilitate the establishment of endocardial atrial myocyte orientation variability, as well as the key functional aspect of change in  $AR_{CV}$  under different pathological conditions. Further data regarding typical myocyte orientation and  $AR_{CV}$  with different pathological states, either through structural imaging or a functional assessment, may contribute to a greater understanding of arrhythmia mechanisms responsible for re-entrant arrhythmias, including AF. Furthermore, such information may be helpful to predict, and possibly guide, the effect of specific anti-arrhythmic medication in the context of defined changes in substrate behaviour. Such an assessment may also allow the identification of regions, for example, those with markedly increased anisotropic conduction, that could be targeted for ablative therapy. Accurate information regarding myocyte orientation and CV anisotropy in an individual atrium would allow a more thorough assessment of the relationship between imaging features (e.g. late-gadolinium enhancement MRI) and functional electrophysiological behaviour, which has rarely been incorporated into previous assessments.<sup>90</sup> It would also allow the parameterisation of patient-specific computational models that may be used to guide individualised precision therapy.

## Conclusion

Myocyte orientation and CV anisotropy are fundamental tissue properties that are important determinants of susceptibility to arrhythmia. Myocyte orientation determines the direction of maximal CV. The ratio between CV in the direction of maximal and minimal CV, the  $AR_{CV}$  represents a determinant of tissue susceptibility to re-entry through the promotion of UCB. In addition, anisotropic conduction itself represents a mechanism that may explain the existence of functional re-entry within cardiac tissue. Tools for establishing myocyte orientation and conduction anisotropy *in vivo* may address outstanding questions regarding the magnitude and mechanism underlying changes in conduction anisotropy in pro-arrhythmic pathologies. ■

## Clinical Perspective

- Tissue anisotropy is dependent on myocyte orientation.
- Anisotropic myocardial conduction is enhanced in pathological states, which may contribute to arrhythmogenesis, through the promotion of abnormal focal activation, as well as functional re-entrant arrhythmias.
- If identifiable during clinical procedures, areas of enhanced anisotropic conduction may represent novel targets in which ablative therapy could be trialled if demonstrated to promote fibrillation.



1. Knisley SB. Transmembrane voltage changes during unipolar stimulation of rabbit ventricle. *Circ Res* 1995;77:1229–39. <https://doi.org/10.1161/01.RES.77.6.1229>; PMID: 7586236.
2. Efimov IR, Gray RA, Roth BJ. Virtual electrodes and deactivation: new insights into fibrillation induction and defibrillation. *J Cardiovasc Electrophysiol* 2000;11:339–53. <https://doi.org/10.1111/j.1540-8167.2000.tb01805.x>; PMID: 10749359.
3. Sano T, Talayama N, Shimamoto T. Directional difference of conduction velocity in the cardiac ventricular syncytium studied by microelectrodes. *Circ Res* 1959;7:262–7. <https://doi.org/10.1161/01.RES.7.2.262>; PMID: 13629828.
4. Valderrábano M. Influence of anisotropic conduction properties in the propagation of the cardiac action potential. *Prog Biophys Mol Biol* 2007;94:144–68. <https://doi.org/10.1016/j.pbiomolbio.2007.03.014>; PMID: 17482242.
5. Hooks DA, Trew ML, Caldwell BJ, et al. Laminar arrangement of ventricular myocytes influences electrical behavior of the heart. *Circ Res* 2007;101:103–12. <https://doi.org/10.1161/CIRCRESAHA.107.161075>; PMID: 17947797.
6. Caldwell BJ, Trew ML, Sands GB, et al. Three distinct directions of intramural activation reveal nonuniform side-to-side electrical coupling of ventricular myocytes. *Circ Arrhythmia Electrophysiol* 2009;2:433–40. <https://doi.org/10.1161/CIRCEP.108.830133>; PMID: 19808500.
7. Smith AF, Shipley RJ, Lee J, et al. Transmural variation and anisotropy of microvascular flow conductivity in the rat myocardium. *Ann Biomed Eng* 2014;42:1966–77. <https://doi.org/10.1007/s10439-014-1028-2>; PMID: 24866569.
8. Wang K, Ho SY, Gibson DG, et al. Architecture of atrial musculature in humans. *Heart* 1995;73:559–65. <https://doi.org/10.1136/hrt.73.6.559>; PMID: 7626357.
9. Kleber A, Rudy Y. Basic mechanisms of cardiac impulse propagation and associated arrhythmias. *Physiol Rev* 2004;84:431–88. <https://doi.org/10.1152/physrev.00025.2003>; PMID: 15044680.
10. Knisley SB, Hill BC. Effects of bipolar point and line stimulation in anisotropic rabbit epicardium: assessment of the critical radius of curvature for longitudinal block. *IEEE Trans Biomed Eng* 1995;42:957–66. <https://doi.org/10.1109/10.464369>; PMID: 8582725.
11. Greenbaum RA, Ho SY, Gibson DG, et al. Left ventricular fiber architecture in man. *Br Heart J* 1981;45:248–63. <https://doi.org/10.1136/hrt.45.3.248>; PMID: 7008815.
12. Ho SY, Sánchez-Quintana D. The importance of atrial structure and fibers. *Clin Anat* 2009;22:52–63. <https://doi.org/10.1002/ca.20634>; PMID: 18470938.
13. Clerc BYL. Directional differences of impulse spread in trabecular muscle from mammalian heart. 1976;255:335–46. <https://doi.org/10.1113/j.physiol.1976.sp011283>; PMID: 1255523.
14. Roberts DE, Scher AM. Effect of tissue anisotropy on extracellular potential fields in canine myocardium in situ. *Circ Res* 1982;50:342–51. <https://doi.org/10.1161/01.RES.50.3.342>; PMID: 7060230.
15. Plonsey R, Henriquez C, Trayanova N. Extracellular (volume conductor) effect on adjoining cardiac muscle electrophysiology. *Med Biol Eng Comput* 1988;26:126–9. <https://doi.org/10.1007/BF02442253>; PMID: 3226166.
16. Spach MS. The discontinuous nature of electrical propagation in cardiac muscle. *Ann Biomed Eng* 1983;11:208–61. <https://doi.org/10.1007/BF02363287>; PMID: 6670785.
17. Tung L. A Bidomain model for describing ischaemic myocardial c-p potentials. Thesis. Massachusetts Institute of Technology, Department of Electrical Engineering and Computer Science. 1978:277.
18. Henriquez CS. Simulating the electrical behavior of cardiac tissue using the bidomain model. *Crit Rev Biomed Eng* 1993;21:1–77. PMID: 8365198.
19. Roth BJ. How the anisotropy of the intracellular and extracellular conductivities influences stimulation of cardiac muscle. *J Math Biol* 1992;30:633–46. <https://doi.org/10.1007/BF00948895>; PMID: 1640183.
20. Rohr S, Salzberg BM. Discontinuities in action potential propagation along chains of single ventricular myocytes in culture: multiple site optical recording of transmembrane voltage (MSORTV) suggests propagation delays at the junctional sites between cells. *Biol Bull* 1992;183:342–3. <https://doi.org/10.1086/BBLv183n2p342>; PMID: 29300657.
21. Fast VG, Kleber AG. Microscopic conduction in cultured strands of neonatal rat heart cells measured with voltage-sensitive dyes. *Circ Res* 1993;73:914–25. <https://doi.org/10.1161/01.RES.73.5.914>; PMID: 8403261.
22. Spach MS, Heidlage JF, Dolber PC, et al. Electrophysiological effects of remodeling cardiac gap junctions and cell size. Experimental and model studies of normal cardiac growth. *Circ Res* 2000;86:302–11. <https://doi.org/10.1161/01.RES.86.3.302>; PMID: 10679482.
23. Kong P, Christia P, Frangogiannis NG. The pathogenesis of cardiac fibrosis. *Cell Mol Life Sci* 2014;71:549–74. <https://doi.org/10.1007/s00018-013-1349-6>; PMID: 23649149.
24. De Jong S, Van Veen TAB, Van Rijen HVM, et al. Fibrosis and cardiac arrhythmias. *J Cardiovasc Pharmacol* 2011;57: 630–8. <https://doi.org/10.1097/FJC.0b013e318207a35f>; PMID: 21150449.
25. Kawara T, Derksen R, De Groot JR, et al. Activation delay after premature stimulation in chronically diseased human myocardium relates to the architecture of interstitial fibrosis. *Circulation* 2001;104:3069–75. <https://doi.org/10.1161/hc5001.100833>; PMID: 11748102.
26. Koura T, Hara M, Takeuchi S, et al. Anisotropic conduction properties in canine atria analyzed by high-resolution optical mapping: Preferential direction of conduction block changes from longitudinal to transverse with increasing age. *Circulation* 2002;105:2092–8. <https://doi.org/10.1161/01.CIR.0000015506.36371.0D>; PMID: 11980690.
27. De Bakker JMT, Van Capelle FJL, Janse MJ, et al. Slow conduction in the infarcted human heart: "zigzag" course of activation. *Circulation* 1993;88:915–26. <https://doi.org/10.1161/01.CIR.88.3.915>; PMID: 8353918.
28. Spach MS, Dolber PC, Heidlage JF. Influence of the passive anisotropic properties on directional differences in propagation following modification of the sodium conductance in human atrial muscle. A model of reentry based on anisotropic discontinuous propagation. *Circ Res* 1988;62:811–32. <https://doi.org/10.1161/01.RES.62.4.811>; PMID: 2450697.
29. Fleischhauer J, Lehmann L, Kléber AG. Electrical resistances of interstitial and microvascular space as determinants of the extracellular electrical field and velocity of propagation in ventricular myocardium. *Circulation* 1995;92:587–94. <https://doi.org/10.1161/01.CIR.92.3.587>; PMID: 7634473.
30. Veeraghavan R, Gourdie RG, Poelzing S. Mechanisms of cardiac conduction: a history of revisions. *Am J Physiol Heart Circ Physiol* 2014;306:H619–27. <https://doi.org/10.1152/ajpheart.00760.2013>; PMID: 24414064.
31. Kitamura H, Ohnishi Y, Yoshida A, et al. Heterogeneous loss of connexin43 protein in nonischemic dilated cardiomyopathy with ventricular tachycardia. *J Cardiovasc Electrophysiol* 2002;13:865–70. <https://doi.org/10.1046/j.1540-8167.2002.00865.x>; PMID: 12380923.
32. Fontes MSC, Van Veen TAB, De Bakker JMT, et al. Functional consequences of abnormal Cx43 expression in the heart. *Biochim Biophys Acta* 2012;1818:2020–9. <https://doi.org/10.1016/j.bbamem.2011.07.039>; PMID: 21839722.
33. Van Rijen HVM, Eckardt D, Degen J, et al. Slow conduction and enhanced anisotropy increase the propensity for ventricular tachyarrhythmias in adult mice with induced deletion of connexin43. *Circulation* 2004;109:1048–55. <https://doi.org/10.1161/01.CIR.0000117402.70689.75>; PMID: 14967725.
34. Peters NS, Coromilas J, Severs NJ, et al. Disturbed connexin43 gap junction distribution correlates with the location of reentrant circuits in the epicardial border zone of healing canine infarcts that cause ventricular tachycardia. *Circulation* 1997;95:988–96. <https://doi.org/10.1161/01.CIR.95.4.988>; PMID: 9054762.
35. Gollub MH, Jones DL, Krahn AD, et al. Somatic mutations in the connexin 40 gene (GJA5) in atrial fibrillation. *N Engl J Med* 2006;354:2677–88. <https://doi.org/10.1056/NEJMoa052800>; PMID: 16790700.
36. Thibodeau IL, Xu J, Li Q, et al. Paradigm of genetic mosaicism and lone atrial fibrillation: physiological characterization of a connexin 43-deletion mutant identified from atrial tissue. *Circulation* 2010;122:236–44. <https://doi.org/10.1161/CIRCULATIONAHA.110.961227>; PMID: 20606116.
37. Igarashi T, Finet JE, Takeuchi A, et al. Connexin gene transfer preserves conduction velocity and prevents atrial fibrillation. *Circulation* 2012;125:216–25. <https://doi.org/10.1161/CIRCULATIONAHA.111.053272>; PMID: 22158756.
38. Akar FG, Tomaselli GF. Conduction abnormalities in nonischemic dilated cardiomyopathy: basic mechanisms and arrhythmic consequences. *Trends Cardiovasc Med* 2005;15:259–64. <https://doi.org/10.1016/j.tcm.2005.08.002>; PMID: 16226681.
39. Zhuang B, Sirajuddin A, Wang S, et al. Prognostic value of T1 mapping and extracellular volume fraction in cardiovascular disease: a systematic review and meta-analysis. *Heart Fail Rev* 2018;23:723–31. <https://doi.org/10.1007/s10741-018-9718-8>; PMID: 29968223.
40. Veeraghavan R, Salama ME, Poelzing S. Interstitial volume modulates the conduction velocity–gap junction relationship. *Am J Physiol Heart Circ Physiol* 2012;302:278–86. <https://doi.org/10.1152/ajpheart.00868.2011>; PMID: 22021331.
41. Cohen SA. Immunocytochemical localization of rhl sodium channel in adult rat heart atria and ventricle: presence in terminal intercalated disks. *Circulation* 1996;94:3083–6. <https://doi.org/10.1161/01.CIR.94.12.3083>; PMID: 8989112.
42. Kucera JP, Rohr S, Rudy Y. Localization of sodium channels in intercalated disks modulates cardiac conduction. *Circ Res* 2002;91:1176–82. <https://doi.org/10.1161/01.RES.0000046237.54156.0A>; PMID: 12480819.
43. Aijjola OA, Lux RL, Khaheera A, et al. Sympathetic modulation of electrical activation in normal and infarcted myocardium: implications for arrhythmogenesis. *Am J Physiol Heart Circ Physiol* 2017;312:H608–21. <https://doi.org/10.1152/ajpheart.00575.2016>; PMID: 28087519.
44. Kelly A, Salerno S, Connolly A, et al. Normal interventricular differences in tissue architecture underlie right ventricular susceptibility to conduction abnormalities in a mouse model of Brugada syndrome. *Cardiovasc Res* 2018;114:724–36. <https://doi.org/10.1093/cvr/cvx244>; PMID: 29267949.
45. Noorman M, Hakim S, Kessler E, et al. Remodeling of the cardiac sodium channel, connexin43, and plakoglobin at the intercalated disk in patients with arrhythmogenic cardiomyopathy. *Heart Rhythm* 2013;10:412–9. <https://doi.org/10.1016/j.hrthm.2012.11.018>; PMID: 23178689.
46. James TN. The internodal pathways of the human heart. *Prog Cardiovasc Dis* 2001;43:495–535. <https://doi.org/10.1053/pcad.2001.24598>; PMID: 11431803.
47. Wagner ML, Lazzara R, Weiss RM, et al. Specialized conducting fibers in the interatrial band. *Circ Res* 1966;18:502–18. <https://doi.org/10.1161/01.RES.18.5.502>; PMID: 5937541.
48. Li-jun J, Xue-yin L, Cong-xin H, et al. Electrophysiologic characteristics of the crista terminalis and implications on atrial tachycardia in rabbits. *Cell Biochem Biophys* 2012;62:267–71. <https://doi.org/10.1007/s12013-011-9290-5>; PMID: 21938558.
49. Spach MS, Miller WT, Geselowitz DB, et al. The discontinuous nature of propagation in normal canine cardiac muscle. Evidence for recurrent discontinuities of intracellular resistance that affect the membrane currents. *Circ Res* 1981;48:39–54. <https://doi.org/10.1161/01.RES.48.1.39>; PMID: 7438345.
50. Maesen B, Zeemering S, Afonso C, et al. Rearrangement of atrial bundle architecture and consequent changes in anisotropy of conduction constitute the 3-dimensional substrate for atrial fibrillation. *Circ Arrhythm Electrophysiol* 2013;6:967–75. <https://doi.org/10.1161/CIRCEP.113.000050>; PMID: 23969531.
51. Morton JB, Sanders P, Vohra JK, et al. Effect of chronic right atrial stretch on atrial electrical remodeling in patients with an atrial septal defect. *Circulation* 2003;107:1775–82. <https://doi.org/10.1161/01.CIR.0000058164.68127.F2>; PMID: 12665497.
52. Kupersmith J, Kronrad E, Waldo AL. Conduction intervals and conduction velocity in the human cardiac conduction system. Studies during open-heart surgery. *Circulation* 1973;47:776–85. <https://doi.org/10.1161/01.CIR.47.4.776>; PMID: 4696799.
53. Boyden PA. Purkinje physiology and pathophysiology. *J Interv Card Electrophysiol* 2018;52:255–62. <https://doi.org/10.1007/s10840-018-0414-3>; PMID: 30056516.
54. Ono N, Yamaguchi T, Ishikawa H, et al. Morphological varieties of the Purkinje fiber network in mammalian hearts, as revealed by light and electron microscopy. *Arch Histol Cytol* 2009;72:139–49. <https://doi.org/10.1007/s00408-009-0072-1>; PMID: 20513977.
55. Schaliq MJ, Lammers WJEP, Rensma PL, et al. Anisotropic conduction and reentry in perfused epicardium of rabbit left ventricle. *Am J Physiol Heart Circ Physiol* 1992;263:H1466–78. <https://doi.org/10.1152/ajpheart.1992.263.5.H1466>; PMID: 1279990.
56. Rijcken J, Bovendeerd PHM, Schoofs AJG, et al. Optimization of cardiac fiber orientation for homogeneous fiber strain at beginning of ejection. *J Biomech* 1997;30:1041–9. [https://doi.org/10.1016/S0021-9290\(97\)00664-X](https://doi.org/10.1016/S0021-9290(97)00664-X); PMID: 9391871.
57. Wong CX, John B, Brooks AG, et al. Direction-dependent conduction abnormalities in the chronically stretched atria. *Europace* 2012;14:954–61. <https://doi.org/10.1093/europace/eur428>; PMID: 22308090.
58. Krul SPJ, Berger WR, Smit NW, et al. Atrial fibrosis and conduction slowing in the left atrial appendage of patients undergoing thoracoscopic surgical pulmonary vein isolation for atrial fibrillation. *Circ Arrhythm Electrophysiol* 2015;8:288–95. <https://doi.org/10.1161/CIRCEP.114.001752>; PMID: 25673630.
59. Glukhov AV, Fedorov VV, Kalish PW, et al. Conduction remodeling in human end-stage nonischemic left ventricular cardiomyopathy. *Circulation* 2012;125:1835–47. <https://doi.org/10.1161/CIRCULATIONAHA.111.047274>; PMID: 22412072.
60. Anter E, Tschabrunn CM, Buxton AE, et al. High-resolution mapping of postinfarction reentrant ventricular tachycardia: electrophysiological characterization of the circuit. *Circulation* 2016;134:314–27. <https://doi.org/10.1161/CIRCULATIONAHA.116.021955>; PMID: 27440005.
61. Mayer A. Rhythmic pulsation in scyphomedusa. Washington DC, US: Carnegie Institute of Washington; 1906:1–62.
62. Rudy Y. Reentry: insights from theoretical simulations in a fixed pathway. *J Cardiovasc Electrophysiol* 1995;6:294–312. <https://doi.org/10.1111/j.1540-8167.1995.tb00402.x>; PMID: 7544193.
63. Quan W, Rudy Y. Unidirectional block and reentry of cardiac excitation: a model study. *Circ Res* 1990;66:367–82. <https://doi.org/10.1161/01.RES.66.2.367>; PMID: 2297808.
64. Ciaccio EJ, Coromilas J, Ashikaga H, et al. Model of unidirectional block formation leading to reentrant ventricular tachycardia in the infarct border zone of postinfarction canine hearts. *Comput Biol Med* 2015;62:254–63. <https://doi.org/10.1016/j.combiomed.2015.04.032>; PMID: 25966920.
65. Mehra R, Zeiler RH, Gough WB, et al. Reentrant ventricular arrhythmias in the late myocardial infarction period. 9. Electrophysiological and anatomic correlation of reentrant circuits. *Circulation* 1983;67:11–24. <https://doi.org/10.1161/01.CIR.67.1.11>; PMID: 6183020.
66. Wit AL, Allesse MA, Bonke FIM, et al. Electrophysiological mapping to determine the mechanism of experimental ventricular tachycardia initiated by premature impulses. Experimental approach and initial results demonstrating



- reentrant excitation. *Am J Cardiol* 1982;49:166–85. [https://doi.org/10.1016/0002-9149\(82\)90292-2](https://doi.org/10.1016/0002-9149(82)90292-2); PMID: 6172033.
67. Allesie MA, Bonke FIM, Schopman FJG. Circus movement in rabbit atrial muscle as a mechanism of tachycardia II. The role of nonuniform recovery of excitability in the occurrence of unidirectional block, as studied with multiple electrodes. *Circ Res* 1976;41:9–18. <https://doi.org/10.1161/01.RES.41.1.9>; PMID: 862147.
  68. Shaw RM, Rudy Y. Ionic mechanisms of propagation in cardiac tissue. Roles of the sodium and L-type calcium currents during reduced excitability and decreased gap junction coupling. *Circ Res* 1997;81:727–41. <https://doi.org/10.1161/01.RES.81.5.727>; PMID: 9351447.
  69. Delgado C, Steinhaus B, Delmar M, et al. Directional differences in excitability and margin of safety for propagation in sheep ventricular epicardial muscle. *Circ Res* 1990;67:97–110. <https://doi.org/10.1161/01.RES.67.1.97>; PMID: 2364498.
  70. Allesie MA, Bonke FI, Schopman FJ. Circus movement in rabbit atrial muscle as a mechanism of tachycardia. III. The "leading circle" concept: a new model of circus movement in cardiac tissue without the involvement of an anatomical obstacle. *Circ Res* 1977;41:9–18. <https://doi.org/10.1161/01.RES.41.1.9>; PMID: 862147.
  71. Gough WB, Mehra R, Restivo M, et al. Reentrant ventricular arrhythmias in the late myocardial infarction period. 13. Correlation of activation and refractory maps. *Circ Res* 1985;57:432–42. <https://doi.org/10.1161/01.RES.57.3.432>; PMID: 4028346.
  72. Cherry EM, Ehrlich JR, Nattel S, et al. Pulmonary vein reentry--properties and size matter: insights from a computational analysis. *Heart Rhythm* 2007;4:1553–62. <https://doi.org/10.1016/j.hrthm.2007.08.017>; PMID: 18068635.
  73. Haissuguere M, Jais P, Shah D, et al. Spontaneous initiation of atrial fibrillation by ectopic beats originating in the pulmonary veins. *N Engl J Med* 1998;33:659–66. <https://doi.org/10.1056/NEJM199809033391003>; PMID: 9725923.
  74. Schaliq MJ, Boersma L, Huijberts M, et al. Anisotropic reentry in a perfused 2-dimensional layer of rabbit ventricular myocardium. *Circulation* 2000;102:2650–58. <https://doi.org/10.1161/01.CIR.102.21.2650>; PMID: 11085970.
  75. Ho SY, Sanchez-Quintana D, Cabrera JA, et al. Anatomy of the left atrium: implications for radiofrequency ablation of atrial fibrillation. *J Cardiovasc Electrophysiol* 1999;10:1525–33. <https://doi.org/10.1111/j.1540-8167.1999.tb00211.x>; PMID: 10571372.
  76. Dierckx H, Bernus O, Verschelde H. A geometric theory for scroll wave filaments in anisotropic excitable media. *Phys D Nonlinear Phenom* 2009;238:941–50. <https://doi.org/10.1016/j.physd.2008.09.006>.
  77. Pravdin S, Dierckx H, Markhasin VS, et al. Drift of scroll wave filaments in an anisotropic model of the left ventricle of the human heart. *Biomed Res Int* 2015;389830. <https://doi.org/10.1155/2015/389830>; PMID: 26539486.
  78. Qu Z, Kil J, Xie F, et al. Scroll wave dynamics in a three-dimensional cardiac tissue model: roles of restitution, thickness, and fiber rotation. *Biophys J* 2000;78:2761–75. [https://doi.org/10.1016/S0006-3495\(00\)76821-4](https://doi.org/10.1016/S0006-3495(00)76821-4); PMID: 10827961.
  79. Allesie MA, Schaliq MJ, Kirchhof CJHJ, et al. Electrophysiology of spiral waves in two dimensions: the role of anisotropy. *Ann N Y Acad Sci* 1990;591:247–56. <https://doi.org/10.1111/j.1749-6632.1990.tb15093.x>; PMID: 2197923.
  80. Efimov IR, Sidorov V, Cheng Y, et al. Evidence of three-dimensional scroll waves with ribbon-shaped filament as a mechanism of ventricular tachycardia in the isolated rabbit heart. *J Cardiovasc Electrophysiol* 1999;10:1452–62. <https://doi.org/10.1111/j.1540-8167.1999.tb00204.x>; PMID: 10571365.
  81. Valderrábano M, Lee MH, Ohara T, et al. Dynamics of intramural and transmural reentry during ventricular fibrillation in isolated swine ventricles. *Circ Res* 2001;88:839–48. <https://doi.org/10.1161/01.RES.88.8.839>; PMID: 11325877.
  82. Bishop MJ, Plank G. The role of fine-scale anatomical structure in the dynamics of reentry in computational models of the rabbit ventricles. *J Physiol* 2012;590:4515–35. <https://doi.org/10.1113/jphysiol.2012.229062>; PMID: 22753546.
  83. Spach MS, Miller WT, Dolber PC, et al. The functional role of structural complexities in the propagation of depolarization in the atrium of the dog. Cardiac conduction disturbances due to discontinuities of effective axial resistivity. *Circ Res* 1982;50:175–91. <https://doi.org/10.1161/01.RES.50.2.175>; PMID: 7055853.
  84. Witkowski F, Leon L, Penkoske P, et al. Spatiotemporal evolution of ventricular fibrillation. *Nature* 1998;392:78–82. <https://doi.org/10.1038/32170>; PMID: 9510250.
  85. Wilders R, Wagner MB, Golod DA, et al. Effects of anisotropy on the development of cardiac arrhythmias associated with focal activity. *Pflügers Arch* 2000;441:301–12. <https://doi.org/10.1007/s004240000413>; PMID: 11211117.
  86. Pashkhanloo F, Herzka DA, Mori S, et al. Submillimeter diffusion tensor imaging and late gadolinium enhancement cardiovascular magnetic resonance of chronic myocardial infarction. *J Cardiovasc Magn Reson* 2017;19:9. <https://doi.org/10.1186/s12968-016-0317-3>; PMID: 28122618.
  87. McGill LA, Ismail TF, Nielles-Vallespin S, et al. Reproducibility of in-vivo diffusion tensor cardiovascular magnetic resonance in hypertrophic cardiomyopathy. *J Cardiovasc Magn Reson* 2012;14:86. <https://doi.org/10.1186/1532-429X-14-86>; PMID: 23259835.
  88. Ariga R, Tunncliffe EM, Manohar SG, et al. Identification of myocardial disarray in patients with hypertrophic cardiomyopathy and ventricular arrhythmias. *J Am Coll Cardiol* 2019;73:2493–502. <https://doi.org/10.1016/j.jacc.2019.02.065>; PMID: 31118142.
  89. Roney CH, Whitaker J, Sim I, et al. A technique for measuring anisotropy in atrial conduction to estimate conduction velocity and atrial fibre direction. *Comput Biol Med* 2019;104:278–90. <https://doi.org/10.1016/j.combiomed.2018.10.019>; PMID: 30415767.
  90. Fukumoto K, Habibi M, Ipek EG, et al. Association of left atrial local conduction velocity with late gadolinium enhancement on cardiac magnetic resonance in patients with atrial fibrillation. *Circ Arrhythm Electrophysiol* 2016;9:e002897. <https://doi.org/10.1161/CIRCEP.115.002897>; PMID: 26917814.
  91. Keith A, Flack M. The form and nature of the muscular connections between the primary divisions of the vertebrate heart. *J Anat Physiol* 1907;41:172–89. PMID: 1723272.